Bridging the gap

Spiekman, Maroesjka

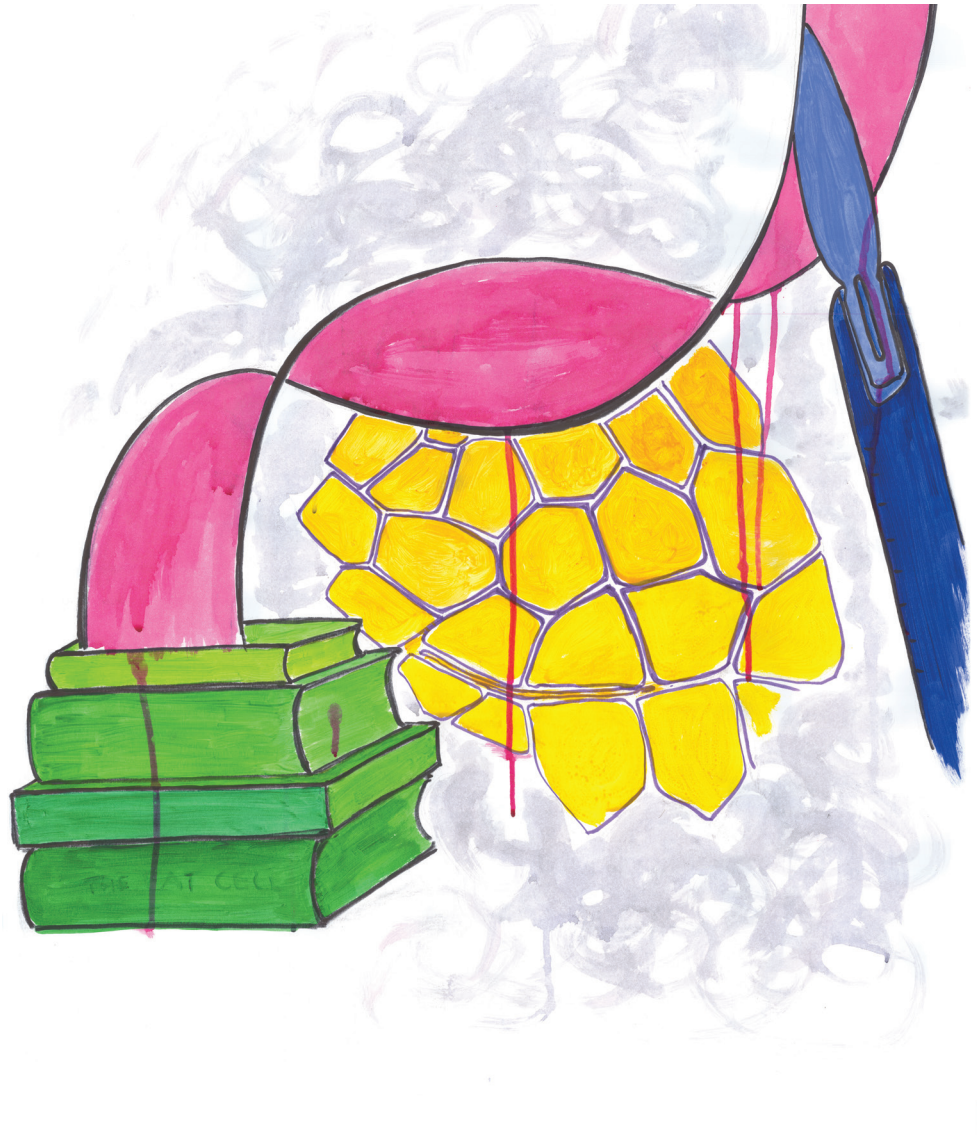

CHAPTER 3

Autologous lipofilling improves clinical outcome in patients with symptomatic dermal scars through induction of a pro-regenerative immune response

Maroesjka Spiekman [1], Delia L. Hoppe [2], Dieuwertje M. Mossel [3], Linda A. Brouwer [1], Gilles F.H. Diercks [1], Karin M. Vermeulen [4], Mark Folkertsma [1], Mojtaba Ghods [2], Michael Walter [5,6], Julia Kzhyshkowska[3,7], Harald Klüter [3,7], Guido Krenning [1], Berend van der Lei [8,9], Martin C. Harmsen [1]

1. Department of Pathology and Medical Biology, University of Groningen, University Medical Center Groningen, Groningen, The Netherlands
2. Department of Plastic and Reconstructive Microsurgery / Hand Surgery, Charité University Medicine, Ernst Von Bergmann Clinic, Potsdam, Germany
3. Institute of Transfusion Medicine and Immunology, Medical Faculty Mannheim, University of Heidelberg, Mannheim, Germany
4. Department of Epidemiology, University of Groningen, University Medical Center Groningen, The Netherlands
5. Institute of Laboratory Medicine, Clinical Chemistry and Pathobiochemistry, Campus Virchow Klinikum, Charité, University Medicine, Berlin, Germany
6. Labor Berlin, Charité Vivantes Services GmbH, Berlin, Germany
7. German Red Cross Blood Service Baden-Württemberg-Hessen, Mannheim, Germany
8. Department of Plastic Surgery, University of Groningen, University Medical Center Groningen, Groningen, The Netherlands Bergman Clinics Heerenveen and Zwolle, The Netherlands

Submitted for publication

ABSTRACT

Background

Treatment of symptomatic dermal scars is challenging and frequently unsuccessful. Recently, autologous lipofilling emerged as a promising therapy because it improves scar quality (*e.g.* elasticity) and often reduces scar-related pain. However, evidence for clinical efficacy is scarce and the biological mechanisms induced by lipofilling that underlie improved clinical outcome and supposed scar remodeling remain elusive.

Methods

In a prospective, non-placebo controlled clinical therapeutic study, 20 adult patients with symptomatic scars were treated with two consecutive lipofilling treatments at three-month intervals. As primary outcome, clinical effects were evaluated using the Patient and Observer Scar Assessment Scale (POSAS). Scar biopsies were taken before and after treatments to assess vessel density, epidermal proliferation, extracellular matrix (ECM) organization, and immune cell content. Influence of paracrine immune signaling was investigated *in vitro* via angiogenesis assays.

Results

Patients' scars improved after both lipofilling treatments, as reflected by a decrease in total POSAS scores from 73.2±14.7 points pre-treatment to 46.1±14.0 ($p<0.001$) and 32.3±13.2 ($p<0.001$) after the first and second treatment, respectively. After lipofilling treatments, T lymphocytes, mast cells and M2 macrophages had extensively invaded scar tissues and this was accompanied by increased vascularization. *In vitro*, the secreted factors of mast cells and M2 macrophages induced vessel formation. In addition, the scar-associated epidermis showed improved regenerative capacity as indicated by considerable increase in epidermal cell proliferation. Moreover, lipofilling treatment caused normalization of ECM organization towards that of normal skin.

Conclusion

Autologous lipofilling improves clinical outcome of dermal scars through the induction of a pro-regenerative immune response, increased vascularization, and epidermal proliferation and remodeling of scar tissue ECM**.**

INTRODUCTION

To date, treatment of symptomatic dermal scars is challenging and frequently does not sufficiently reduce scar visibility and associated pathological symptoms[1]. Dermal scarring results from adverse wound healing, meaning it must always begin with damage to the skin. Upon progression through the well-known steps of wound healing (*i.e.* inflammation, new tissue formation and remodeling), this healing process normally resolves by fibrosis. In normal physiology, the epidermis and dermis are subsequently restored[2].

The resolution of wound healing results in a scar that might be indistinguishable from normal skin (normotrophic) or may acquire pathological features such as in the case of hypertrophic and keloid scars[3], which cause clinical symptoms[1,3]. Even though these pathological scars give rise to complaints far more often than normotrophic scars, normotrophic scars may also cause symptoms. With regard to symptoms, we will use the terms physiological versus symptomatic scar.

Visibility of dermal scars due to reduced aesthetics and differences in color and texture as compared to normal skin burdens the patient. In addition, volume defects may exist *e.g.* in burn wound scars or degloving injuries[4]. Moreover, scars may be painful, itchy, and in certain cases cause functional impairment by movement restriction[1].

Lipofilling, the subcutaneous administration of processed autologous lipoaspirates, is a promising therapy for scars because it adjusts volume defects caused by scars and improves scar quality *e.g.* elasticity[5,6]. Finally, lipofilling is known to reduce neuropathy via an unknown mechanism and also appears to reduce scar-related pain[7]. Unfortunately, published observations on the influence of lipofilling are poorly controlled and virtually all lack mechanistic insight.

From a biological perspective, it remains elusive why lipofilling leads to such observed clinical improvements, including improvement of the aesthetic aspect, normalization of tissue elasticity, and reduction of scar-related pain. Therefore, the current study was undertaken to evaluate the clinical outcome of lipofilling on symptomatic scars that were resistant to conventional scar therapy and to unravel the underlying histological changes that may explain its mechanism.

MATERIALS AND METHODS

Experimental design

This study was approved by the medical ethical committees of both centers involved (reference numbers 256/2014MPG23 and 167/2015MPG43). All patients that agreed to participate in this study gave their written informed consent prior to inclusion in the study. The design of the study is a prospective, non-placebo controlled therapeutic study. Adult patients with symptomatic scars existing longer than six months, or with scars existing less than six months causing significant functional impairment (*e.g.* decreased mobility across joints) were included in this study. There

were no other treatment options available for these patients. All inclusion and exclusion criteria are listed in Table 1. Patients suitable for inclusion in this study were invited to participate. Patients were included at the departments of Plastic, Reconstructive, Hand and Burn Surgery, BG-Trauma Center, Eberhard Karls University, Tübingen, Germany, and the Department of Plastic and Reconstructive Microsurgery and Handsurgery, Charité University Medicine, Ernst Von Bergmann Clinic, Potsdam, Germany. Outcome measures (see below) were recorded prior to any lipofilling treatment and three months after the initial treatment. Then, another lipofilling treatment was performed and final evaluation took place six months after the initial treatment. A detailed diagram of the study is outlined in Figure 1.

Lipofilling treatment

The lipofilling treatment (minimally invasive scar release combined with water jet-assisted autologous lipofilling) was performed as described previously[8,9] with modifications. All procedures were performed under general anesthesia. All treatments were performed by the same surgeon (DLH) to reduce variations between operations. Lipoaspirates were harvested with the Water Jet-Assisted Liposuction System (Humanmed AG, Schwerin, Germany) from either the abdomen or inner thighs. To begin, a standard Klein's tumescence solution was infiltrated. Lipoaspirates were harvested with liposuction cannulas (Humanmed AG, Schwerin, Germany) and collected in the Lipocollector System (Humanmed AG, Schwerin, Germany) according to the previously described method[10-12]. After processing, the obtained lipoaspirates were administered into the scar area. The volume of lipoaspirate injected into the each scar related to the surface area and depth of the scar, based on clinical judgement and experience. Postoperative, standard compression dressings were used to compress the donor area. The scar area was immobilized when possible and custom made cushioning dressing was applied to decrease stress and pressure on the injected lipoaspirate. All patients received antibiotics for five days.

Clinical assessment

As the primary outcome measure, the Patient and Observer Scar Assessment Scale (POSAS) – a validated questionnaire to evaluate the severity of scarring[13] – was used. POSAS questionnaires

Table 1 | In- and exclusion criteria for study patients

Inclusion criteria	Exclusion criteria
Age > 18 years; Patients with symptomatic scars with complaints existing for >6 months, which do not respond to conventional therapy* Patients with scars with complaints <6 months can also be included in case of progressive, movement restricting scars and/or contractures.	Age <18 years; Pregnancy or active child wish; A known psychiatric condition; A known cardiac condition; Alcohol abuse; Weight changes (>5kg in 2 months).

*I.e. Silicon sheet treatment, compression therapy, scar creams and operative scar revision

were filled out before lipofilling, three months after the first lipofilling treatment and three months after the second lipofilling treatment. The Observer scales were filled out by the same observer (DLH). Total POSAS scores were calculated by summing the scores of all items of the Patient and Observer questionnaires, except for the item 'overall opinion'. Complications were also monitored during the entire follow-up period.

Tissue collection and preservation

Three consecutive scar biopsies were obtained from all patients: just before the moment of the first lipofilling treatment (intra-operative), three months after the first treatment and three months after the second lipofilling treatment. The incisions remaining from the biopsies were subsequently used as the entrance port for lipofilling. The last (third) biopsy was taken under local anesthesia with Xylocaine 1% with adrenalin (1:200,000) using a biopsy punch. Lipoaspirates were collected from six patients from the Lipocollector System after completion of the lipofilling treatment Immediately after collection, tissues were formalin fixed and then paraffin embedded. For Adipose derived stromal cells (ASC) isolation, lipoaspirates were preserved at 4°C until start of the isolation procedure.

Lipoaspirate immunohistochemistry

Lipoaspirates were stained with antibodies for αSMA (ab7817, Abcam, Cambridge, UK), von Willebrand Factor (vWF, A0082, Dako, Glostrup, Denmark) and perilipin (ab3526, Abcam, Cambridge, UK). As secondary antibodies, Rabbit anti-Mouse and consecutively with Swine anti-Rabbit peroxidase conjugated antibodies (P0260 and P0217, Dako, Glostrup, Denmark) for αSMA, Swine anti-Rabbit peroxidase conjugated antibody (P0217, Dako, Glostrup, Denmark) for vWF or Goat anti-Rabbit peroxidase conjugated antibody (P0448, Dako, Glostrup, Denmark) for perilipin were used. Paraffin embedded samples were sectioned at 10µm. Slides were incubated at 60°C overnight and tissues were deparaffinnized afterwards. Antigen retrieval was performed using a 0.1M Tris/HCL buffer overnight at 80°C (αSMA and perilipin) or by microwaving in 10mM Tris with 1mM EDTA buffer for 4 minutes (vWF). Endogenous peroxidases were blocked with 30% hydrogen peroxide solution. Afterwards, tissue slices were washed and incubated with primary antibodies diluted 1:200 in PBS with 1% human serum (for αSMA and perilipin) or 1% swine serum (for vWF) and 1% bovine serum albumin (BSA; Sigma-Aldrich, St. Louis, MO) for 1 hour. After extensive washing, tissue sections were incubated with secondary antibodies diluted 1:100 in in PBS with 1% human serum and 1% BSA, for 30 minutes. For antigen detection, tissues were incubated with diaminobenzidine (DAB) in the dark for 10 minutes. All tissues were counterstained with hematoxylin and mounted in Aquatex (Merkc, Darmstadt, Germany). For quantification, slides were scanned with the NanoZoomer 2.0-HT slide scanner (Hamamatsu, Hersching am Ammersee, Germany) and analyzed using the Positive Pixel Count algorithm version 9 in the Aperio ImageScope Software version 12.1 (Leica Biosystems, Nussloch, Germany).

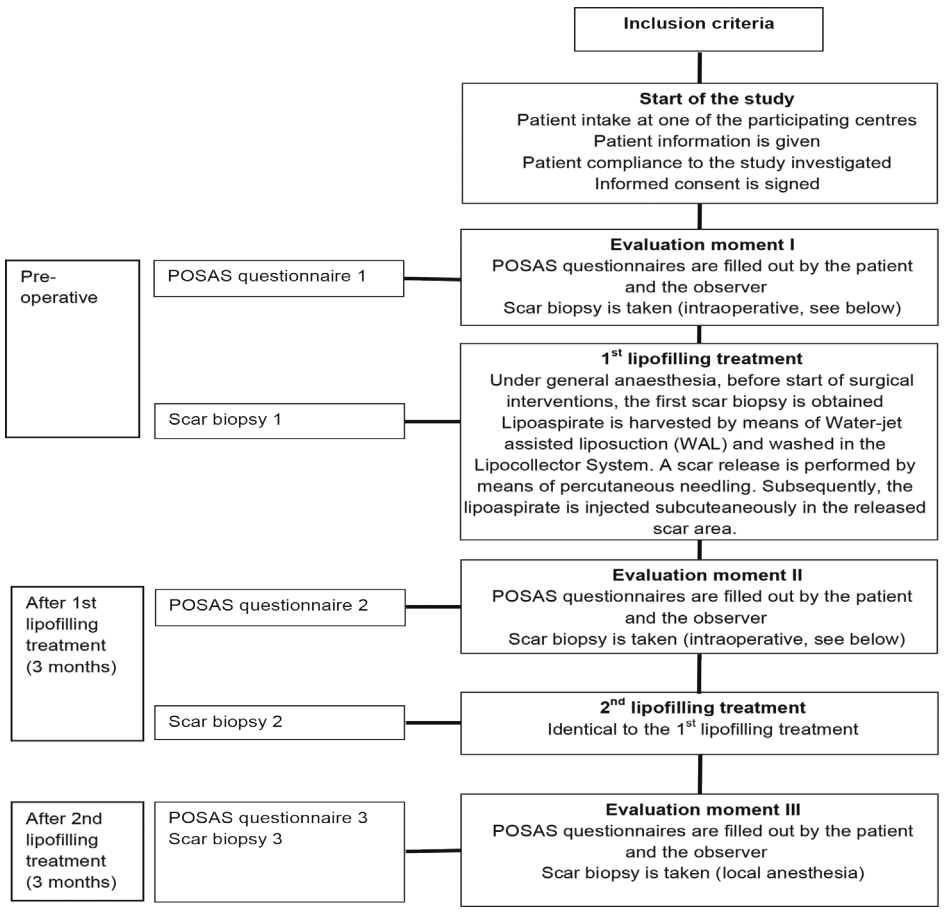

Figure 1 | Study flow diagram

Adipose derived stromal cell isolation and characterization

ASC were isolated from the lipoaspirate of five study patients. The lipoaspirates were washed with phosphate buffered saline (PBS) and were dissociated enzymatically with 0.1% Collagenase A (Roche Diagnostic, Mannheim, Germany) in PBS with 1% BSA (Sigma-Aldrich, St. Louis, MO) at 37°C for one hour. The digested tissue was centrifuged and the supernatant containing oil and adipocytes was discarded. Pellets were collected, washed and subjected to a density gradient centrifugation step using Lymphoprep (Axis Shield PoC, Oslo, Norway). The stromal vascular fraction (SVF) was collected from the interphase and was treated with erythrocyte lysis buffer on ice for 10 minutes. Cell number and viability were determined using a Bürker-Turk counting chamber and trypan blue. The freshly isolated SVF cells were plated at a density of $8x10^4$ cells per cm^2 in Dulbecco's Modified Eagle's Medium (DMEM; Lonza, Breda, The Netherlands) containing

10% fetal bovine serum (FBS; GE Lifesciences, Piscataway, NJ), 2mM L-glutamine (Sigma-Aldrich, St. Louis, MO) and 1% penicillin/streptomycin (Sigma-Aldrich, St. Louis, MO). After 24 hours, non-adherent cells were washed away. The remaining ASC were cultured to approximately 95% confluency, before passaging. Characterization of surface marker expression, differentiation and Colony Forming Unit (CFU) assays were performed at passage 3.

For assessment of CFU potential, 10 or 100 cells per cm^2 were seeded in triplicate and cultured for fourteen days. Afterwards, cells were fixed with 2% paraformaldehyde (PFA) and stained with 0.05% Crystal Violet (Sigma-Aldrich, St. Louis, MO). Culture plates were scanned using a Zeiss Axio Observer.Z1 microscope (Carl Zeiss, Mainz, Germany) in light microscopy mode. Surface area covered by colonies and colony intensity was calculated using ImageJ (National Institutes of Health, Bethesda, MD) and the ColonyArea plugin, as described by Guzman *et al.*[14].

For differentiation assays, near confluent layers of ASC were cultured with control medium (DMEM with 10% FBS, 2mM L-glutamine and 1% penicillin/streptomycin) or with differentiation media for three weeks. Adipogenic differentiation medium consisted of control medium supplemented with 0.1µM dexamethasone (Sigma-Aldrich, St. Louis, MO), 0.5mM 3-Isobutyl-1-methylxanthine (IBMX; Sigma-Aldrich, St. Louis, MO) and 1nM Insulin (Sigma-Aldrich, St. Louis, MO). Osteogenic differentiation medium consisted of control medium supplemented with 0.1µM dexamethasone, 10mM β-glycerophosphate (Sigma-Aldrich, St. Louis, MO) and 0.05mM ascorbic acid (Sigma-Aldrich, St. Louis, MO). Myogenic differentiation medium consisted of control medium with 10ng/mL of recombinant human TGF-β1 (Peprotech, Rocky Hill, NJ). Cells were fixed with 2% PFA and were assessed for differentiation. For adipogenic differentiation, lipid accumulation was visualized using 0.15% Oil Red O (Sigma-Aldrich, St. Louis, MO) in a 60% isopropanol solution. Osteogenic differentiation was assessed by visualizing mineralization using a 40mM Alizarin Red S (Sigma-Aldrich, St. Louis, MO) solution. Cells were counterstained using hematoxylin. Images were acquired using a Leica DM IL microscope (Leica Microsystems GmbH, Wetzlar, Germany) and a Canon EOS 350D camera (Canon Inc., Tokyo, Japan). Myogenic differentiation was assessed by visualizing polymerized F-actin using Phalloidin-TRITC (Sigma-Aldrich, St. Louis, MO). Images were acquired using a using a Zeiss Axio Observer.Z1 microscope in fluorescence mode.

For characterization of surface marker expression, ASC were detached using Trypsin-EDTA in PBS. Cells were pelleted by centrifugation, washed with PBS and incubated with directly labeled antibodies on ice for 30 minutes. Two sets of antibodies were used. The first set consisted of CD31-Pe/Cy7 (eBioscience #25-0319-41, San Diego, CA), CD45-FITC (IQ-products #IQP-124F, Groningen, The Netherlands) and CD90-APC (BD Biosciences #561971, San Jose, CA). The second set consisted of CD29-APC (eBioscience #17-0299-41, San Diego, CA), CD44-FITC (BD Biosciences #555478, San Jose, CA) and CD105-Pe/Cy7 (eBioscience #25-1057-41, San Diego, CA). Mouse IgG1 kappa-Pe/Cy7, Mouse IgG1 kappa-APC (both eBioscience #25-4714-41 San Diego, CA) and Mouse IgG1 kappa-

FITC (Biolegend #400108, San Diego, CA) were used as isotype controls. Samples were analyzed by flow cytometry on a FACS Calibur (BD Biosciences, San Jose, CA).

Scar tissue immunohistochemistry

Scar tissue biopsies were stained with antibodies for Ki67 (clone 30-9), CD3 (clone 2GV6), tryptase (clone G3) (all from Roche Diagnostics, Mannheim, Germany), CD163 (clone MRQ-26) and alpha smooth muscle actin (αSMA; clone 1A4) (both from Cell Marque, Rocklin, CA). Tissues were sectioned at 5µm, incubated at 80°C overnight and deparaffinized afterwards. All immunohistochemical stainings were performed using a Bench Mark Ultra automated immunostainer (Ventana Medical Systems Inc., Tucson, AZ). Antigen retrieval was performed using Ultra CC1 buffer. Slides were incubated with pre-diluted primary antibody solutions. For antigen detection, the OptiView IHC detection kit (Ventana Medical Systems Inc., Tucson, AZ) was used. For αSMA and CD163, this signal was amplified using the OptiView amplification kit (Ventana Medical Systems Inc., Tucson, AZ). All tissues were counterstained with hematoxylin and mounted using xylene and TissueTek Film (Sakura Finetek, The Netherlands). For quantification, scar tissues were examined using a Leica DM 2000 LED microscope (Leica Microsystems GmbH, Wetzlar, Germany). In four fields of view at 40x magnification (combined surface area of one mm^2), the number of positive cells and the number of vessels were scored by a blinded observer. For Ki67, only cells in the epidermis were scored.

Scar tissue extracellular matrix analyses

Scar tissues were sectioned at 3µm and deparaffinized. Tissues were stained with Weigert's hematoxylin (Sigma Aldrich, St. Louis, MO) and washed extensively with tap water. Afterwards, tissues were stained with Picrosirius Red Solution, consisting of 0.1% (w/v) Direct Red (Sigma Aldrich, St. Louis, MO) in a saturated solution of 1.3% picric acid in water (Sigma Aldrich, St. Louis, MO) for 10 minutes. Then, sections were washed with acidified water, dehydrated with 100% ethanol, and mounted in Permount mounting medium (Sigma Aldrich, St. Louis, MO). Slides were examined using an Olympus BX50 (Olympus Optical Co., Hamburg, Germany) equipped with a linear polarization filter at 10x magnification.

Conditioned medium collection

Conditioned medium (CM) for endothelial sprouting assays was collected from primary isolated human macrophages and from the human mast cell line HMC-1 clone 5C6. Human macrophages were isolated from buffy coats from five individual donors as described previously[15] with modifications. Ficoll and Percoll gradients were centrifuged at 420 g for 30 min at RT without brakes. For the culture, $CD14^+$ monocytes were resuspended in X-Vivo 10 serum free medium (Lonza, Verviers, Belgium) at a concentration of $1x10^6$ cells/mL. The cell suspension was supplemented with 5ng/mL MCSF (Peprotech, Rocky Hill, NJ), 10ng/mL IL-4 (Peprotech, Rocky Hill, NJ) and $1x10^{-8}$ M dexamethasone (Sigma-Aldrich, Munich, Germany) to induce M2 macrophage polarization. The cells were incubated in the presence of 7.5% CO2 for 12 days. The conditioned

media were then harvested and centrifuged to eliminate the intact cells. HMC-1 cells were cultured in Iscove's Modified Dulbecco's Medium (IMDM; Thermo Fisher Scientific, Bremen, Germany) supplemented with 10% FBS, 1% penicillin/streptomycin and 50µM β-mercaptoethanol (Sigma-Aldrich, St. Louis, MO). For CM collection, cells were switched to Roswell Park Memorial Institute (RPMI) 1640 medium (Lonza, Verviers, Belgium) containing 3% FBS, 1% penicillin/streptomycin, and 2mM L-glutamine. HMC-1 cells were maintained in this medium for 24 hours. Afterwards, HMC-1 CM was collected. After collection, all CM were centrifuged to remove cell debris and stored at -20°C until further use.

Endothelial sprouting assay

Human umbilical vein endothelial cells (HUVEC; Lonza, Verviers, Belgium) were used to assess influence of M2 macrophage and mast CM on sprouting. HUVEC culture and endothelial sprouting assays were performed as described previously[16]. As control medium, RPMI 1640 medium containing 3% FBS, 1% penicillin/streptomycin and 2mM L-glutamine or X-vivo 10 medium supplemented with 5ng/mL MCSF, 10ng/mL IL-4 and $1x10^{-8}$ M dexamethasone were used, respectively. Endothelial sprouting was assessed after six hours using light microscopy images, which were analyzed using ImageJ and the Angiogenesis Analyzer, as described by Fortenberry *et al.*[17]. For all conditions, triplicates were analyzed for tube formation. Sprouting assays were performed in duplicate for both M2 macrophage and mast cell CM.

Statistical analysis

All data are represented as mean±SD, unless stated otherwise. The normal distribution of data was tested using the Kolmogorov-Smirnov Test. Normal distributed data were analyzed using a repeated measures one-way analysis of variance (ANOVA) with a Bonferroni post-hoc test unless stated otherwise. Missing data was not imputed. For statistical analyses, GraphPad Prism version 5 (GraphPad Software Inc., La Jolla, CA) and IBM SPSS Statistics 22 (IBM Corp., Armonk, NY) were used. P-values below 0.05 were considered statistically significant.

RESULTS

Patient inclusion

Twenty-seven patients were enrolled in this study and twenty patients completed all lipofilling treatments; eighteen patients completed all POSAS questionnaires, from seventeen patients the series of three scar biopsies was completed (two patients refused the third and final biopsy, of one patient the second biopsy was too small for analyses). Seven patients quit the planned protocol, because of travelling distance (n=3), emergency treatment for a condition not related to the study (n=1) and inability to comply to the study regimen (n=3). Data of patients who dropped out of the study were not included in the analyses.

Patient characteristics

Patient demographics per individual patient are described in Table 2. The average patient age was 49.5±16.1 years. The average patient BMI was 25.4±3.4 kg/m^2. Scars were located in the head and neck area (n=3), on the trunk (n=8), upper extremities (n=4) and lower extremities (n=5). Scars were due to flap harvest (n=4), burns (n=1), necrotizing fasciitis (n=1), a degloving injury (n=3) or were categorized as 'other' surgical scars (n=10). Prior scar treatments consisted of operative scar corrections, scar massage therapy, compression therapy, ergo-therapy, physical therapy, corticosteroid injection and scar creams.

Surgical treatment variables

Forty lipofilling treatments were performed in the course of this study. The average operation time for the entire lipofilling treatments was 75±30 minutes, with a range of 33-155 minutes. The average injected amount of lipoaspirate volume was 71.8±74.3 milliliters per treatment, with a range of 4-355 milliliters. Injected volume depended primarily on clinical judgment and experience related to the surface area and depth of the scar. There was no difference between the average time for the first or second lipofilling treatment nor for the amount of lipoaspirate volume injected at the first or second session of lipofilling (paired t-test, p>0.05).

Complications

Reported donor site sequelae (complications) after liposuction were pain, swelling, bruising, leakage of infiltration fluid from incision sites and hypo or- hyperesthesia. All donor site sequelae resolved spontaneously within a period of one week to one month. In the recipient area of the lipofilling (scar area's to be treated) there was one major complication that required surgery in which a necrotic area of the skin was successfully treated with a skin graft. Two minor complications were reported: a small wound healing problem requiring conservative treatment (regular physician supervised wound irrigations and dressing changes) and a nerve compression in a radial forearm flap donor area requiring conservative treatment (cooling and elevation of graft area, prednisone). None of these complications adversely influenced the POSAS scores or immunohistological results (Two way repeated measures ANOVA, p>0.05).

Clinical improvement of scar appearance after lipofilling treatment

Preoperatively, total POSAS score was 73.2±14.7 points. After the first and second lipofilling treatment, this decreased to 46.1±14.0 and 32.3±13.2 points, respectively (Fig. 2A, p<0.001). The baseline POSAS Observer score was 35.9±9.5 points, which decreased to 18.9±6.0 and 11.3±4.5 points after the first and second lipofilling treatment, respectively (Fig. 2B, p<0.001). For the POSAS Patient scale, pre-operative score was 37.3±8.8 points, which decreased to 27.2±11.3 and 21.1±11.4 points (Fig. 2C, p<0.001 compared to pre-operative score) after the first and second lipofilling treatment, respectively. Though, there was a difference between patient and observer POSAS scores, whereas the mean observer score decreases with 68% where the patient scores decreased by 43% after the second lipofilling treatment as compared to pre-operative (Two

Table 2 | Demographics of the study patients

No.	Gender	Age	Comorbidity*	BMI	Scar location	Trauma / treatment indication	Scar age**	Previous scar therapy
1.	Female	60	None	27.7	Back	Painful scar after lattisimus dorsi flap harvest	2y 3mo	SMT, creams
2.	Female	60	HT	25.8	Knee, lower limb	Countour defect after degloving injury by accident	2y 6mo	SMT, creams, SST
3.	Female	59	None	26.8	Abdomen	Painful scar after DIEP flap harvest	9mo	
4.	Female	52	None	28.4	Neck	Painful, tight scar after thyroidectomy	8y	Operative scar corrections
5.	Female	50	HT	32.9	Lower leg	Painful burn scar with movement restriction	2y 7mo	Operative scar corrections, creams, SST
6.	Female	53	None	21.8	Lower arm	Painful, restrictive scar after fasciotomy for compartment syndrome	7y 9mo	Operative scar corrections, SMT, creams, SST
7.	Female	25	None	23.7	Knee, lower limb	Painful scar with movement restriction after osteosarcoma extirpation	13y	Operative scar corrections
8.	Male	59	HT	28.9	Hand and wrist	Painful, restrictive scar after complex crush injury and amputation	1y	Operative scar corrections, SMT, SST, PT
9.	Female	65	None	28.5	Abdomen	Painful, tight scar after necrotizing fasciitis following abdominoplasty	11mo	Operative scar corrections, creams, SST
10.	Male	83	Pre-DM	30.5	Inguinal/ scrotal region	Painful, progressive scar contracture after scrotal unilateral orchiectomie	5mo	None
11.	Female	76	HT	23.1	Scalp	Painful, depressed scar, after excision of basal cell carcinoma	11y	Operative scar corrections, creams, SMT
12.	Male	26	Smoker	21.2	Inner thigh	Painful scars with movement restriction after gunshot wounds	15y	Operative scar corrections, creams
13.	Female	55	None	21.6	Abdomen	Retracted scar after open appendectomy	33y	None
14.	Male	32	None	28.1	Lower arm	Painful, depressed, restrictive donor area (skin graft) of radial flap	2y 9mo	SMT, SST, creams
15.	Female	53	HT	23.6	Abdomen	Painful scar after laparotomy	44y	Operative scar corrections, creams, SMT, ET

Table 2 (continued) | Demographics of the study patients

No.	Gender	Age	Comorbidity*	BMI	Scar location	Trauma / treatment indication	Scar age**	Previous scar therapy
16.	Male	33	None	20.9	Lower arm	Painful, depressed, restrictive donor area (skin graft) of radial flap	3y 8mo	Operative scar corrections, creams, SMT, SST
17.	Female	34	None	25.6	Temporal region	Painful scar and contour defect after craniotomy	2y 7mo	SMT
18.	Female	42	Smoker	24.4	Sternum	Painful, itching scar after atheroma removal with subsequent infection and secondary healing	1y 4mo	Creams
19.	Female	25	None	20.5	Clavicula	Painful, depressed scar after operative reposition of clavicula fracture	1y 10mo	Operative scar corrections, creams, CI, SST
20.	Female	47	None	24.0	Hand, 4th ray	Painful and depressed scar after amputation following degloving injury	1y	Operative scar corrections, creams, SMT, ET

**Recorded co-morbidities were hypertension, diabetes mellitus (pre-diabetic, type I or II) and smoking*
*** Time since original trauma*

Abbreviations: year (y), months (mo), Hypertension (HT), diabetes mellitus (DM), Scar massage therapy (SMT), Silicon sheet therapy (SST), Physical therapy (PT), Ergotherapy (ET), Corticosteroid injection (CI)

way repeated measures ANOVA, p<0.001). Yet, all POSAS scores (total, patient, and observer) had decreased between the first and second lipofilling treatment (Fig. 2A, B and C, p<0.05).

Lipoaspirate characteristics

From lipoaspirates of five study patients, ASC were isolated and cultured. After culture expansion, these ASC were assessed for surface marker expression, and for differentiation and CFU potential. ASC were $CD90^+$ (99.70±0.22%), $CD44^+$ (98.9±0.97), $CD105^+$ (96.95±1.35%), $CD29^+$ (99.62±0.42%) and $CD45^-$ (99.79±0.09) and $CD31^-$(99.56±0.24) (Supplemental Fig. 1A). As for CFU capacity, after fourteen days of culture with seeding densities of 10 or 100 cells per cm^2, ASC covered 0.28±0.26%

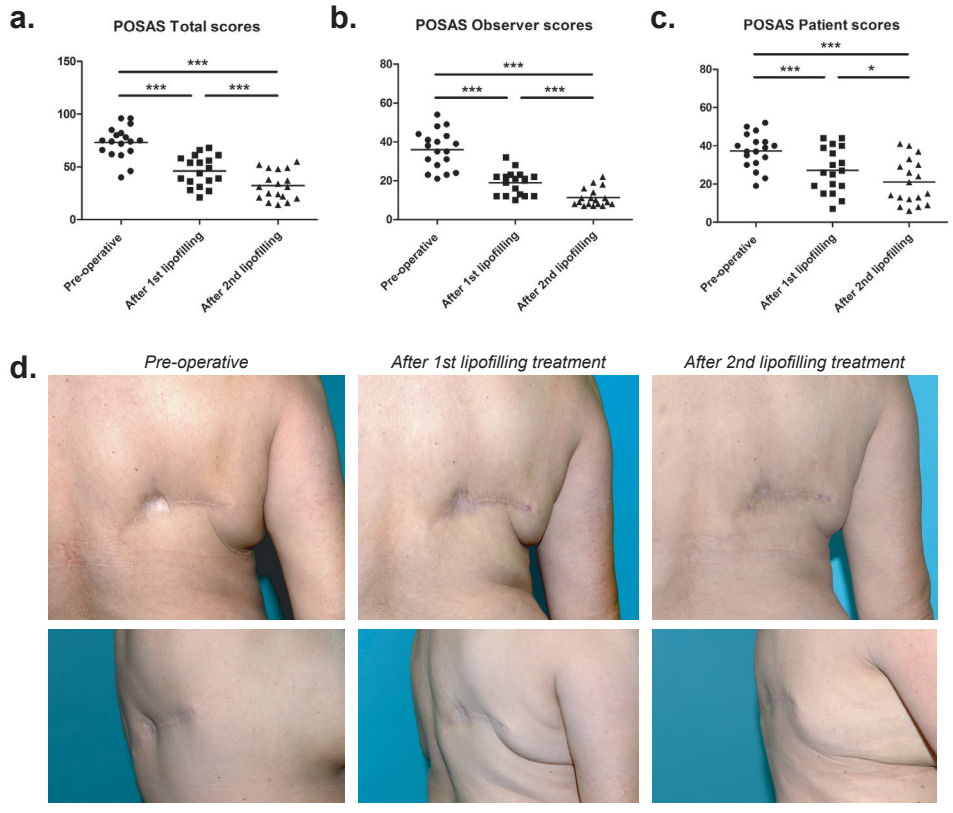

Figure 2 | Lipofilling in symptomatic dermal scars improves clinical outcome, as measured by the POSAS questionnaire (n=18). (A) Total POSAS scores – combination of the scores on all items of the patient and observer scale, except for the item 'overall opinion' (max. total score of 120 for the worst scar imaginable). (B) POSAS scores of the observer scale, consisting of the items vascularity, pigmentation, thickness, relief, pliability and surface area. (C) POSAS scores of the patient scale, combination of scores on the items pain, itch, colour, stiffness, thickness and irregularity. (D) Representative photographs of the scars of a study patient pre-operative, three months after the first lipofilling treatment and three months after the second lipofilling treatment. * P < 0.05, *** P<0.001

and 56.4±22.40% of the surface area, respectively (Supplemental Fig. 1B and C). Furthermore, ASC were able to differentiate into osteoblasts, adipocytes and myogenic cells, as shown by Alizarin Red S, Oil Red O and phalloidin-TRITC staining (Supplemental Fig. 1D). Histologically, the main volume of lipoaspirate fragments comprised of intact adipocytes, while tissue fragments were highly vascularized too (Supplemental Fig. 2). Size of adipocytes appeared normally distributed. Adipose tissue fragments of the lipoaspirates were vascularized, as shown by vWF (endothelial cells) and αSMA (among others mural cells of the vessel wall) positivity in immunochemical analyses.

Increase in epidermal proliferation in scar biopsies after lipofilling

In scar tissues before and after lipofilling, proliferating epidermal cells were located in the basal layer, in a pattern similar to normal skin. Pre-operatively, the number of proliferation cells was 77.8±50.6 positive cells per mm^2, which increased after the first and second treatment of lipofilling to 113.9±47.9 and 124.1±63.1 positive cells per mm^2 (Fig. 3, p<0.05), respectively.

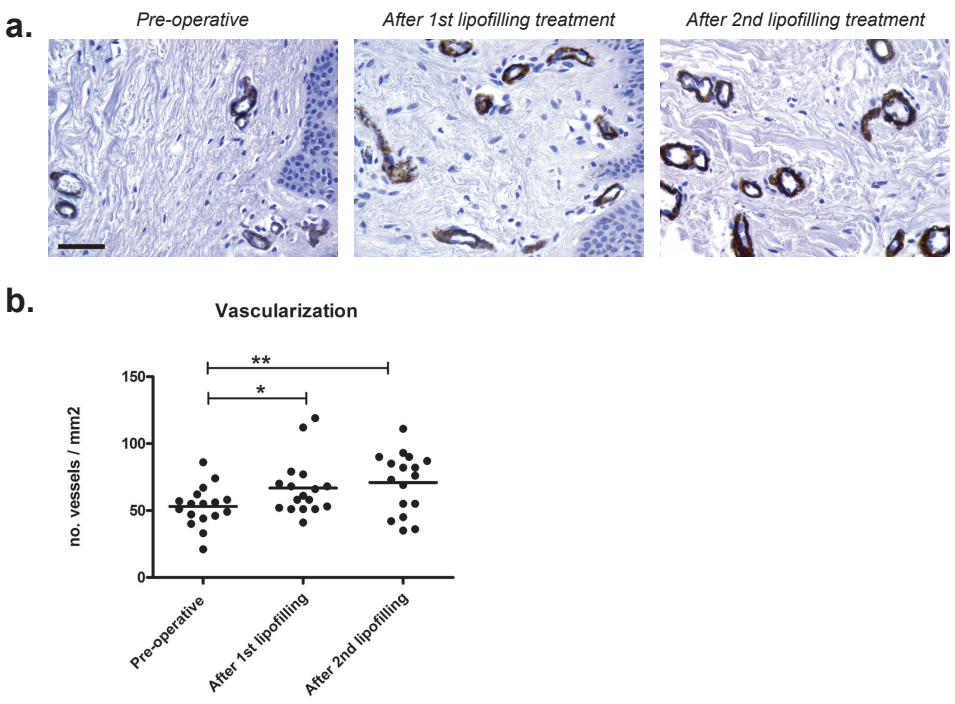

Figure 3 | Epidermal proliferation is increased in scar tissues three months after the first lipofilling treatment and three months after the second lipofilling treatment, as compared to pre-operative. (A) Representative images of immunohistochemical stainings for Ki67 (brown). Scale bar 50µm. (B) Quantification of the number of Ki67 positive cells in the epidermis is four high power fields (n=17). * P< 0.05, ** P < 0.01

Increase in vessel density in scar tissue after lipofilling treatment

Vessel density in scar tissue pre-operatively was 53.0±15.1 vessels per mm^2, which increased to 66.8±21.0 and 70.9±22.5 vessels per mm^2 (Fig. 4, p<0.05) after the first and second lipofilling treatment, respectively.

Increase in immune cells in scar tissue after lipofilling treatment

Numbers of T lymphocytes (CD3), CD163$^+$ (M2 polarized) macrophages and mast cells (tryptase) in scars increased after both the first and the second lipofilling treatment. Pre-operatively, the number of T lymphocytes was 69.0±46.0 per mm^2 of scar tissue, which increased to 138.6±88.2 and 165.9±136.6 (Fig. 5B, p<0.05) after the first and second lipofilling treatment, respectively. The number of CD163$^+$ macrophages was 183.2±107.7 per mm^2 of scar tissue pre-operatively, which increased to 259.7±78.2 per mm^2 (Fig. 5C, p<0.05) of scar tissue after the second lipofilling treatment. The number of mast cells increased from 120.9±56.1 per mm^2 of scar tissue pre-operatively to 161.1±56.3 and 160.1±60.1 per mm^2 (Fig. 5D, p<0.01) after the first and second lipofilling treatment, respectively.

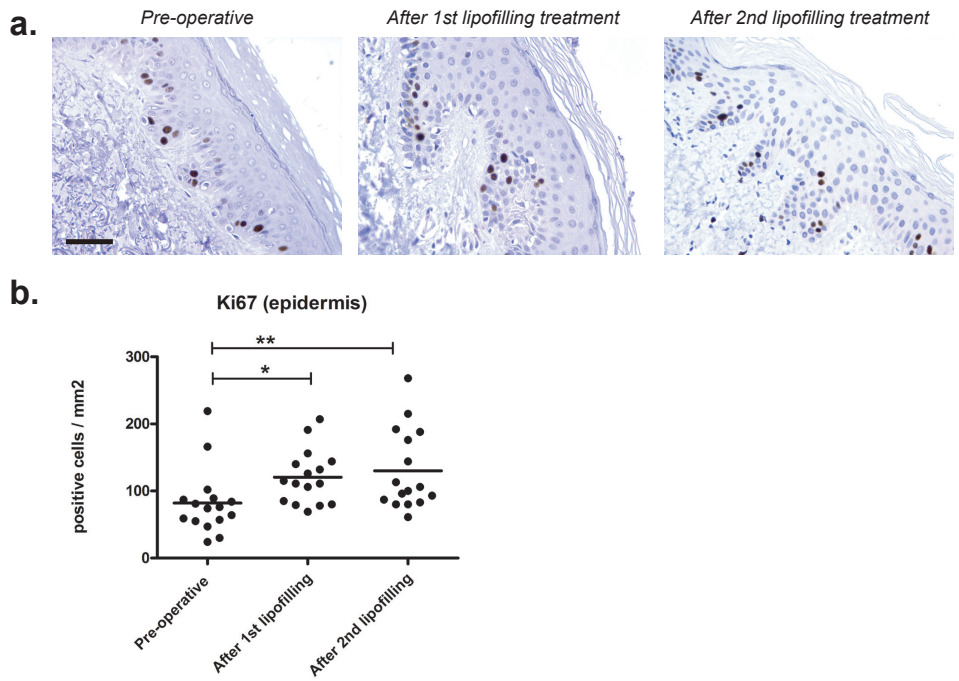

Figure 4 | Vessel density increases in scar tissues three months after the first lipofilling treatment and three months after the second lipofilling treatment, as compared to pre-operative. (A) Representative images of immunohistochemical stainings for αSMA (brown). Scale bar 50µm. (B) Quantification of the number of vessels per mm^2 of scar tissue (n=17). * P< 0.05, ** P < 0.01

M2 macrophage and mast cell conditioned medium increase endothelial sprouting in vitro

Both mast cells and M2 macrophages are known to support and regulate vessel formation *in vivo*[18]. To test whether the increased vessel density after lipofilling could be related to paracrine effects of the invaded immune cells, the pro-angiogenic potency of conditioned culture medium of M2 macrophages and mast cells was assessed in sprouting assays with HUVEC. *In vitro* sprouting was quantified as the number of junctions and the total branch length after six hours of culture on Matrigel. With M2 macrophage conditioned medium and mast cell conditioned medium, the number of junctions was increased by 1.11 and 1.24 fold respectively and the total branch length

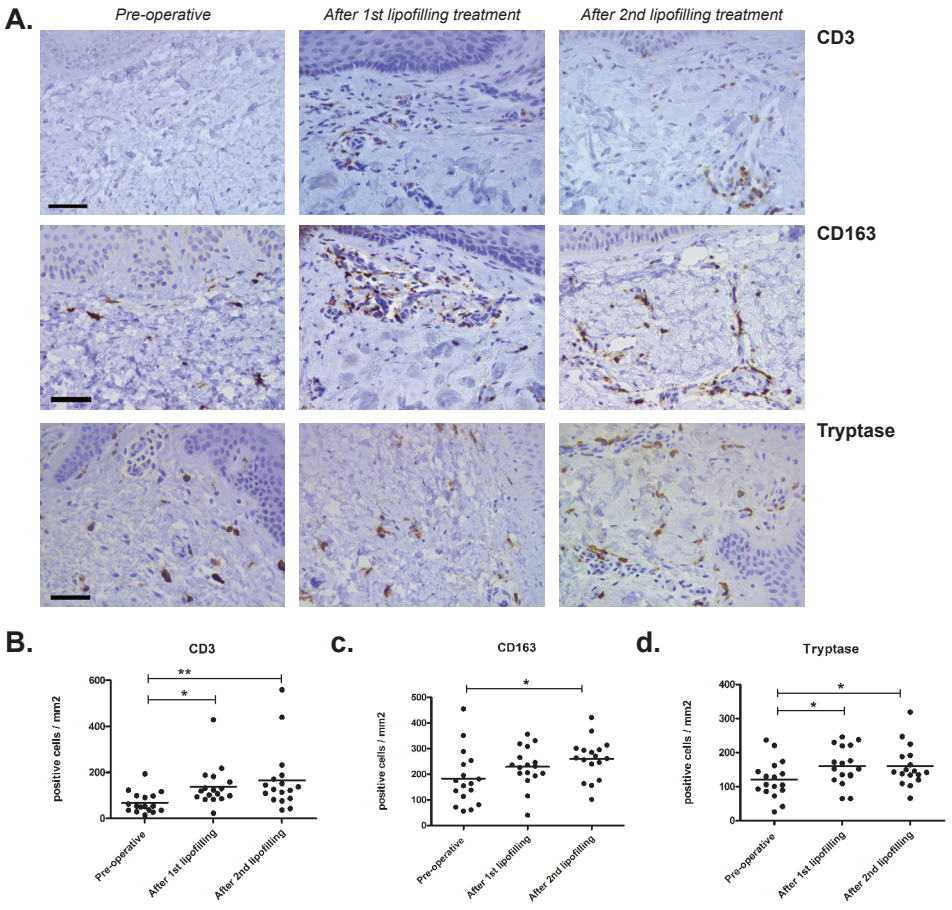

Figure 5 | The number of T lymphocytes, M2 macrophages and mast cells rises in scar tissues three months after the first lipofilling treatment and three months after the second lipofilling treatment, as compared to pre-operative. (A) Representative images for CD3 (T lymphocytes, upper panel), CD163 (M2 macrophages, middle panel) and Tryptase (mast cells, lower panel) immunohistochemical stainings. Scale bars 50µm. Quantification of the number of (B) CD3, (C) CD163 and (D) tryptase positive cells per mm^2 of scar tissue (n=17). * P< 0.05, ** P < 0.01

was increased 1.05 and 1.16 fold respectively, as compared to controls (Fig. 6B, C, E and F, two sided t-test, p<0.05).

Perivascular ECM remodeling in scar tissues after lipofilling treatment

Prior to lipofilling treatment, scar tissues showed classic scar tissue ECM consisting of thick fibrils which aligned parallel to each other and, in most cases, parallel to the epidermis (Fig. 7, left column). ECM of normal skin is distinctly different: it consists of thinner fibers, oriented in a basket-like weave fashion (Fig. 7, right column). After the first lipofilling treatment, slight changes in ECM structure became visible. Around the blood vessels, areas with thinner, non-parallel fibers became visible. Yet, the classical scar tissue ECM organization with thick, parallel fibers was still partially present (Fig. 7, middle left column). After the second lipofilling treatment, an ECM structure with thinner fibers, oriented in a basket weave pattern, became visible in scar tissues from most patients in the vascularized areas (Fig. 7, middle right column).

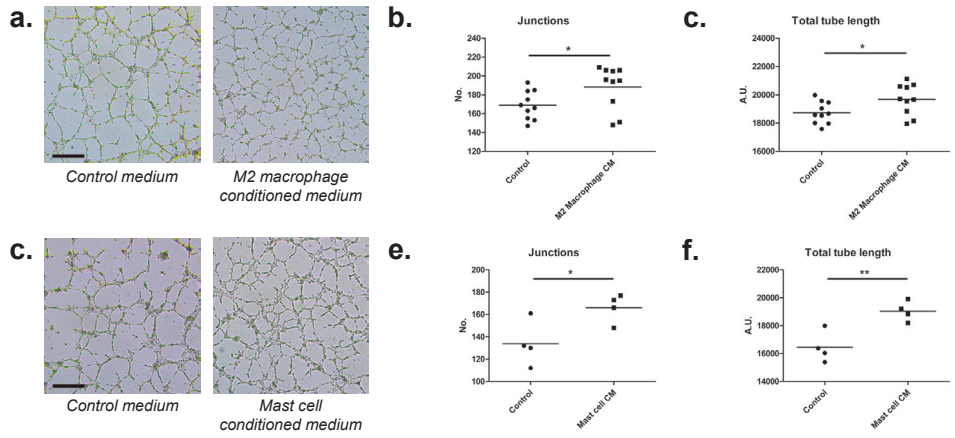

Figure 6 | Trophic factors of M2 macrophages and human mast cell line HMC-1 clone 5C6 are able to stimulate in vitro vessel formation, in a sprouting assay with HUVEC on Matrigel after 6 hours. Representative images of endothelial networks in (A) control medium (left) and in M2 macrophage conditioned medium (right) and (D) control medium (left) and in mast cell conditioned medium. Scale bar 1mm. Quantification of endothelial sprouting in M2 macrophage and mast cell conditioned media as compared to control, depicted as (B, E) number of junctions and (C, F) total branch length. Results represent two independent experiments with conditioned media from five donors (M2 macrophage conditioned media) or from two different HMC-1 cultures (mast cell conditioned media). * P< 0.05, ** P < 0.01

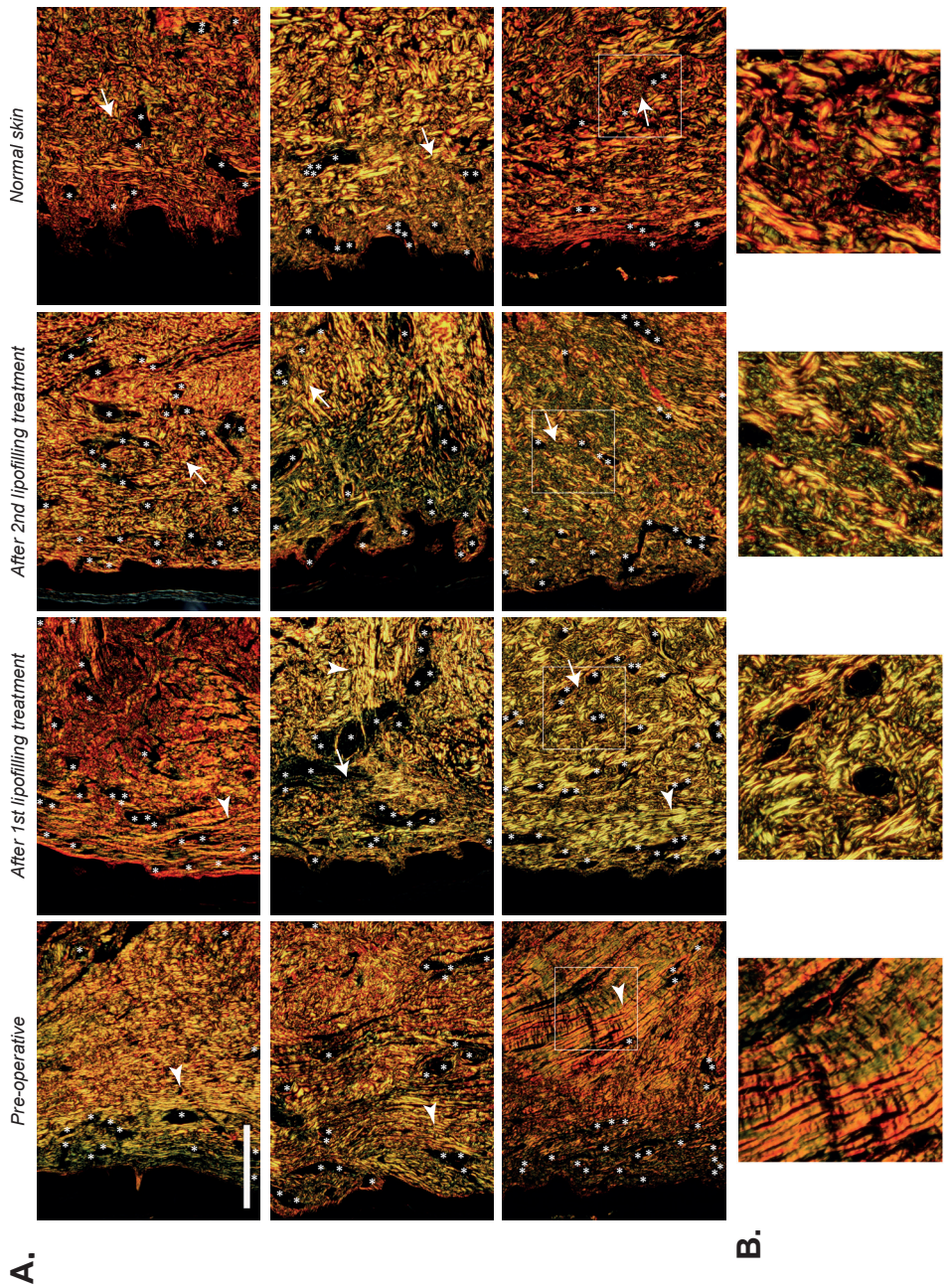

< **Figure 7 |** Lipofilling treatment induces perivascular ECM remodeling in scar tissues. (A) ECM organization of scar tissues – stained with picrosirius red, visualized using polarized light microscopy – of three patients before and after lipofilling is shown, as well as normal skin from three anonymous donors. Note the thick, parallel fibrils (arrowheads) in biopsies from pre-treatment and after the 1st lipofilling. After the 1st and 2nd lipofilling treatment, thinner fibers with a basket weave-like organization (arrows) appear around the vasculature (asterisks). In normal skin, the basket weave-like organization of ECM is uniformly present throughout the tissue (B) Magnification of ECM organization and fibril structure of the last patient. Scale bars 250µm.

DISCUSSION

To the best of our knowledge, this is the first clinical study showing that consecutive sessions of autologous lipofilling lead to marked clinical improvement. This conclusion is based upon several observations. Firstly, the total POSAS score as well as the observer and patients POSAS scores were reduced by up to 80%. This degree of improvement is unique; it is not achieved by any other method in scar treatment. Additionally, clinical improvement was accompanied by positive changes in the scar's microenvironment including vascularization, regeneration of the epidermis, and extracellular matrix remodeling. Furthermore, invasion of T lymphocytes, mast cells, and $CD163^{+}$ (M2 polarized) macrophages point to a pathophysiological explanation for scar release and skin remodeling.

In a recently described study, Jaspers and colleagues[5] found improved elasticity and maximal extension in patients who underwent a single autologous fat grafting treatment. Similar outcomes have been reported by Maione and co-workers[6], who performed lipofilling in pediatric patients with symptomatic scars as a result of surgical limb lengthening. In these patients skin hardness decreased after the procedure. In contrast, Gal and colleagues reported no change in scar quality after lipofilling eight pediatric patients suffering from burn wounds[19], These studies, despite their landmark and pioneering character, had some limitations. No systematic examination of skin histology, texture and cell function was performed; findings were not correlated to cell content of the scars pre- and post-treatment; only a small volume of lipoaspirate was injected in one study, and last but not least, only one lipofilling treatment was performed in each studies. In general, as concluded in two systematic reviews[20,21] and one review[22], the quality of existing study methodology investigating lipofilling for treating scars was low. Thus, evidence for clinical efficacy is currently lacking.

In previous clinical studies, histological changes in scar tissues after lipofilling have been incidentally reported. In a placebo controlled trial carried out by Bruno and co-workers[23], 93 severe burn wound-induced scars were treated with lipofilling on one side and saline injections on the other side. In this study, POSAS scores suggested scar improvement after lipofilling, which coincided with increased proliferation in general in the scar as well as changes in the ECM. These authors show that at least in one patient Langerhans cells (immune sentinel cells in the skin) migrate into

the scar area. Drawbacks of this study were that it is unclear if histological examinations were carried out on biopsies of a single patient, or more patients, and that there were no reported outcomes for the placebo control group. In a case report publication, Klinger *et al.*[24] reported an increase in vessel density and epithelial hyperplasia after lipofilling in the scar tissue of a single patient. Our study corroborates and extends on these results. However, our study is different than the others in that we correlate the clinical finding to the immune cell content of the scars pre- and post-treatment.

In our study, significant clinical improvement in patients with symptomatic scars is accompanied by histological changes of the treated scar tissues that suggest on-going tissue remodeling and normalization (summarized in Fig. 8). According to this concept multiple lipofilling treatments would be superior to a single lipofilling session.

An increase in epidermal proliferation and vessel density was observed after the first and second lipofilling treatment. At later time points, such as six months after initiation of lipofilling treatment, remodeling of ECM structure occurred. Typical scar tissue ECM, consisting of thick, highly-aligned fibrils, was replaced by or transformed into thinner, smaller bundles with a more typical physiological organization. These changes were particularly striking in highly vascularized areas, where the influx of T lymphocytes, mast cells and M2 macrophages has taken place. Thus, changes in immune balance may play an important role in the observed pro-regenerative effect of lipofilling.

It has been suggested that M2 macrophages and mast cells play a critical role in the etiology of pathological scarring: The latter mentioned cells are essential in wound healing in other organs such as the neonatal heart[25] and adult liver[26] and can prevent scar formation in the early stages of fibroproliferative disorders, but M2 macrophages induce fibrosis at later stages. *In vitro* studies with M2 macrophages and dermal fibroblasts demonstrate contradictory results, since either M2 macrophage trophic factors induced myofibroblast differentiation[27] or limited myofibroblast formation[28]. As for mast cells, no difference was found in the number of mast cells when physiological, normotrophic scars were compared to pathological, hypertrophic scars[29,30]. *In vitro* studies regarding mast cell trophic factors, such as tryptase and histamine, show stimulated myofibroblast differentiation and collagen production by dermal fibroblasts[31]. In our *in vitro* experiments, we demonstrated that mast cells as well as M2 macrophages also have pro-regenerative capacities because they promote vessel formation.

The described findings are also of interest from a more general pathophysiological point of view. The role of immune cells in pathological scar formation is under debate: are inflammation and immune cells beneficial or unfavourable for scarless wound healing? In the fetus during the first two trimesters of gestation, absence of an inflammatory reaction results in wound healing without occurrence of scar formation[32]. In addition, the production of the pro-fibrotic

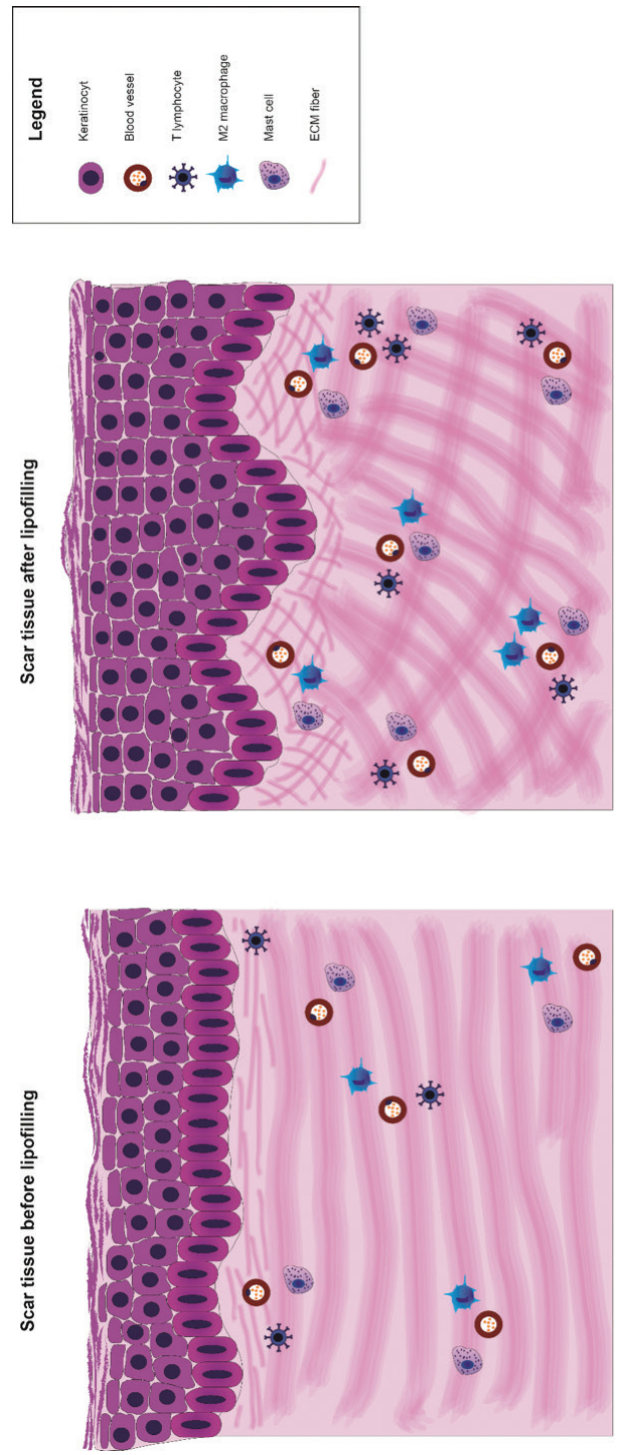

Figure 8 | Schematic overview of histological changes in scar tissues after two consecutive lipofilling treatments. Positive changes in the scar's microenvironment include increase in vascularization, regeneration of the epidermis, and extracellular matrix remodeling. Furthermore, invasion of T lymphocytes, mast cells, and $CD163^{+}$ (M2 polarized) macrophages point to a pathophysiological explanation for scar release and skin remodeling.

chemokine TGF-b1, starts no sooner than the third trimester. On the other hand, recent evidence suggests that regulatory immune cells augment adult wound healing and skin regeneration. In particular the production of FGF9 by γδ T cells is necessary for hair follicle neogenesis after wound healing in mice[33]. Interestingly, the secretion of BMP by hair follicles promotes differentiation of myofibroblasts – key players in scar formation – into adipocytes during resolution of wound healing[34], thus returning the dermal wound to a quiescent state. Adult wound healing, inflammation, and immune cell influx go hand in hand. We surmise that tipping the balance towards a pro-regenerative immune response will lead to prevention or even resolution of dermal scarring.

The depth at which it was possible to take the biopsies, unfortunately did not allow to assess changes in subcutaneous adipose tissue after lipofilling. We do surmise, however, the possibility that part of the adipose-derived stromal cells (ASC) of the lipoaspirate, migrated into the scar to contribute, for example to the attraction of the immune cells since ASC produce both MCP-1 and IL-8 that attract macrophages. Also, ASC secrete pro-angiogenic growth factors such as VEGF-A and FGFs. The lipoaspirates were autologous, which did not allow us to study the fate and function of the administered cells with specific markers. Future studies in animals using reporter-tagged lipoaspirates could shed light on the instructive and directive role of the administered cell preparations.

A limitation of our study is the lack of a placebo control group. We employed a treatment protocol that combines a scar release with lipofilling and did not compare this to only scar release without lipofilling. For several reasons, however, it is very likely that lipofilling substantially contributed to the described scar release process. Many patients were already treated with conventional therapies. The process of scarring was largely completed. In view of this and according to best clinical experience, the improvements were impressive. Based upon our pre- and postoperative histological findings, treatment induced a reversal of scarring. We substantiated the data by a plausible physiological hypothesis, including a pro-regenerative immune response.

CONCLUSION

Our clinical therapeutic study on the use of scar release combined with autologous lipofilling as treatment for symptomatic dermal scars clearly demonstrates clinical value. The treatment results in significant clinical improvement, and is accompanied by the following histological changes in scar tissues: a pro-regenerative immune response, an increase in vascularization and epidermal proliferation, and remodeling of fibrotic scar tissue towards ECM structure resembling normal skin.

CONTRIBUTORS

MS, DLH and MCH designed the clinical study. MS, GK, BvdL and MCH wrote grant applications. DLH and MG were responsible for patient recruitment. MG provided clinical and logistical support

for execution of the clinical trial. DLH performed the surgical procedures. MS and DLH collected clinical data. MS, DMM, LAB, JK, HK, GK and MCH were responsible for design, execution, data collection and evaluation of *in vitro* experiments. MW provided laboratory infrastructure for ASC isolation. MS, LAB, GFHD, MF and MCH conducted and examined histological stainings. MS, GK and MCH analyzed the data and produced all figures and tables. MS, KMV and GK performed statistical analyses. MS, GK, BvdL and MCH drafted the report, all authors contributed to review and revisions. All authors read and approved the final version.

CONFLICT OF INTEREST

We declare that we have no conflict of interest.

FUNDING

This work was funded by the University Medical Center Groningen, University of Groningen, Groningen, the Netherlands, by DFG GRK1874 DIAMICOM, and by grants from Jan-Kornelis de Cock Foundation (to MS), Ubbo Emmius Fund – Junior Scientific Masterclass Talent Grant (to MS) and Foundation “De Drie Lichten” (to MS), the Netherlands. This study was sponsored by Human Med AG, Schwerin, Germany, which provided the Water Jet-Assisted Liposuction System and supplies for this system as well as funds to cover part of the research costs and traveling expenses of DLH.

ACKNOWLEDGEMENTS

The authors would like to thank dr. Lars Morawietz for his cooperation in immunohistochemical analyses, Jacko Duker for arranging the logistics around immunohistochemical stainings, Brigitte Köttgen and Kathrin Jäger for assistance in cell culture and Joris van Dongen for sharing his expertise in ASC characterization.

REFERENCES

1. Aarabi, S., Longaker, M.T. & Gurtner, G.C. Hypertrophic scar formation following burns and trauma: new approaches to treatment. *PLoS Med* **4**, e234 (2007).
2. Gurtner, G.C., Werner, S., Barrandon, Y. & Longaker, M.T. Wound repair and regeneration. *Nature* **453**, 314-321 (2008).
3. van der Veer, W.M.*, et al.* Potential cellular and molecular causes of hypertrophic scar formation. *Burns* **35**, 15-29 (2009).
4. Bayat, A., McGrouther, D.A. & Ferguson, M.W. Skin scarring. *BMJ (Clinical research ed.)* **326**, 88-92 (2003).
5. Jaspers, M.E.*, et al.* Effectiveness of Autologous Fat Grafting in Adherent Scars: Results Obtained by a Comprehensive Scar Evaluation Protocol. *Plast Reconstr Surg* **139**, 212-219 (2017).
6. Maione, L.*, et al.* Autologous fat graft as treatment of post short stature surgical correction scars. *Injury* **45 Suppl 6**, S126-132 (2014).
7. Huang, S.H.*, et al.* Alleviation of neuropathic scar pain using autologous fat grafting. *Ann Plast Surg* **74 Suppl 2**, S99-104 (2015).
8. Hoppe, D.L. Volumendefekte an Stamm und Extremitäten. in *Autologe Fettgewebstransplantation* (ed. Ueberreiter, K.) 113-117 (Springer-Verlag Berlin, 2016).
9. Hoppe, D.L. Verbrennungsnarben. in *Autologe Fettgewebstransplantation* (ed. Ueberreiter, K.) 133-136 (Springer-Verlag, Berlin, 2016).
10. Hoppe, D.L.*, et al.* Breast reconstruction de novo by water-jet assisted autologous fat grafting–a retrospective study. *GMS German Medical Science* **11**(2013).
11. Meyer, J.*, et al.* Isolation and differentiation potential of human mesenchymal stem cells from adipose tissue harvested by water jet-assisted liposuction. *Aesthetic surgery journal* **35**, 1030-1039 (2015).
12. Ueberreiter, K.*, et al.* BEAULI™-A New and Easy Method for Large-Volume Fat Grafts. *Handchirurgie, Mikrochirurgie, plastische Chirurgie* **43**, 65-65 (2011).
13. Draaijers, L.J.*, et al.* The Patient and Observer Scar Assessment Scale: A Reliable and Feasible Tool for Scar Evaluation. *Plast Reconstr Surg* **113**, 1960-1965 (2004).
14. Guzman, C., Bagga, M., Kaur, A., Westermarck, J. & Abankwa, D. ColonyArea: an ImageJ plugin to automatically quantify colony formation in clonogenic assays. *PLoS One* **9**, e92444 (2014).
15. Kzhyshkowska, J.*, et al.* Stabilin-1 localizes to endosomes and the trans-Golgi network in human macrophages and interacts with GGA adaptors. *Journal of leukocyte biology* **76**, 1151-1161 (2004).

16. Correia, A.C., Moonen, J.-R.A., Brinker, M.G. & Krenning, G. FGF2 inhibits endothelial–mesenchymal transition through microRNA-20a-mediated repression of canonical TGF-β signaling. *J Cell Sci* **129**, 569-579 (2016).
17. Fortenberry, Y.M., Brandal, S.M., Carpentier, G., Hemani, M. & Pathak, A.P. Intracellular Expression of PAI-1 Specific Aptamers Alters Breast Cancer Cell Migration, Invasion and Angiogenesis. *PLoS One* **11**, e0164288 (2016).
18. Riabov, V.*, et al.* Role of tumor associated macrophages in tumor angiogenesis and lymphangiogenesis. *The regulation of angiogenesis by tissue cell-macrophage interactions*, 63 (2014).
19. Gal, S., Ramirez, J.I. & Maguina, P. Autologous fat grafting does not improve burn scar appearance: A prospective, randomized, double-blinded, placebo-controlled, pilot study. *Burns* **43**, 486-489 (2017).
20. Negenborn, V.L., Groen, J.W., Smit, J.M., Niessen, F.B. & Mullender, M.G. The Use of Autologous Fat Grafting for Treatment of Scar Tissue and Scar-Related Conditions: A Systematic Review. *Plast Reconstr Surg* **137**, 31e-43e (2016).
21. Conde-Green, A.*, et al.* Fat Grafting and Adipose-Derived Regenerative Cells in Burn Wound Healing and Scarring: A Systematic Review of the Literature. *Plast Reconstr Surg* **137**, 302-312 (2016).
22. Spiekman, M.*, et al.* The power of fat and its adipose-derived stromal cells: emerging concepts for fibrotic scar treatment. *J Tissue Eng Regen Med* (2017).
23. Bruno, A.*, et al.* Burn scar lipofilling: immunohistochemical and clinical outcomes. *J Craniofac Surg* **24**, 1806-1814 (2013).
24. Klinger, M., Marazzi, M., Vigo, D. & Torre, M. Fat injection for cases of severe burn outcomes: a new perspective of scar remodeling and reduction. *Aesthetic Plast Surg* **32**, 465-469 (2008).
25. Aurora, A.B.*, et al.* Macrophages are required for neonatal heart regeneration. *J Clin Invest* **124**, 1382-1392 (2014).
26. Duffield, J.S.*, et al.* Selective depletion of macrophages reveals distinct, opposing roles during liver injury and repair. *J Clin Invest* **115**, 56-65 (2005).
27. Glim, J.E., Niessen, F.B., Everts, V., van Egmond, M. & Beelen, R.H. Platelet derived growth factor-CC secreted by M2 macrophages induces alpha-smooth muscle actin expression by dermal and gingival fibroblasts. *Immunobiology* **218**, 924-929 (2013).
28. Ploeger, D.T.*, et al.* Cell plasticity in wound healing: paracrine factors of M1/ M2 polarized macrophages influence the phenotypical state of dermal fibroblasts. *Cell Commun Signal* **11**, 29 (2013).
29. Niessen, F.B., Schalkwijk, J., Vos, H. & Timens, W. Hypertrophic scar formation is associated with an increased number of epidermal Langerhans cells. *J Pathol* **202**, 121-129 (2004).

30. Beer, T.W., Baldwin, H., West, L., Gallagher, P.J. & Wright, D.H. Mast cells in pathological and surgical scars. *Br J Ophthalmol* **82**, 691-694 (1998).

31. Gailit, J., Marchese, M.J., Kew, R.R. & Gruber, B.L. The differentiation and function of myofibroblasts is regulated by mast cell mediators. *J Invest Dermatol* **117**, 1113-1119 (2001).

32. Xue, M. & Jackson, C.J. Extracellular Matrix Reorganization During Wound Healing and Its Impact on Abnormal Scarring. *Adv Wound Care (New Rochelle)* **4**, 119-136 (2015).

33. Gay, D.*, et al.* Fgf9 from dermal gammadelta T cells induces hair follicle neogenesis after wounding. *Nat Med* **19**, 916-923 (2013).

34. Plikus, M.V.*, et al.* Regeneration of fat cells from myofibroblasts during wound healing. *Science* **355**, 748-752 (2017).

SUPPLEMENTALS

Supplemental figure 1 | Characterization of ASC isolated from lipoaspirates of five representative study patients.

Supplemental figure 2 | Lipoaspirate histology from five representative study patients.

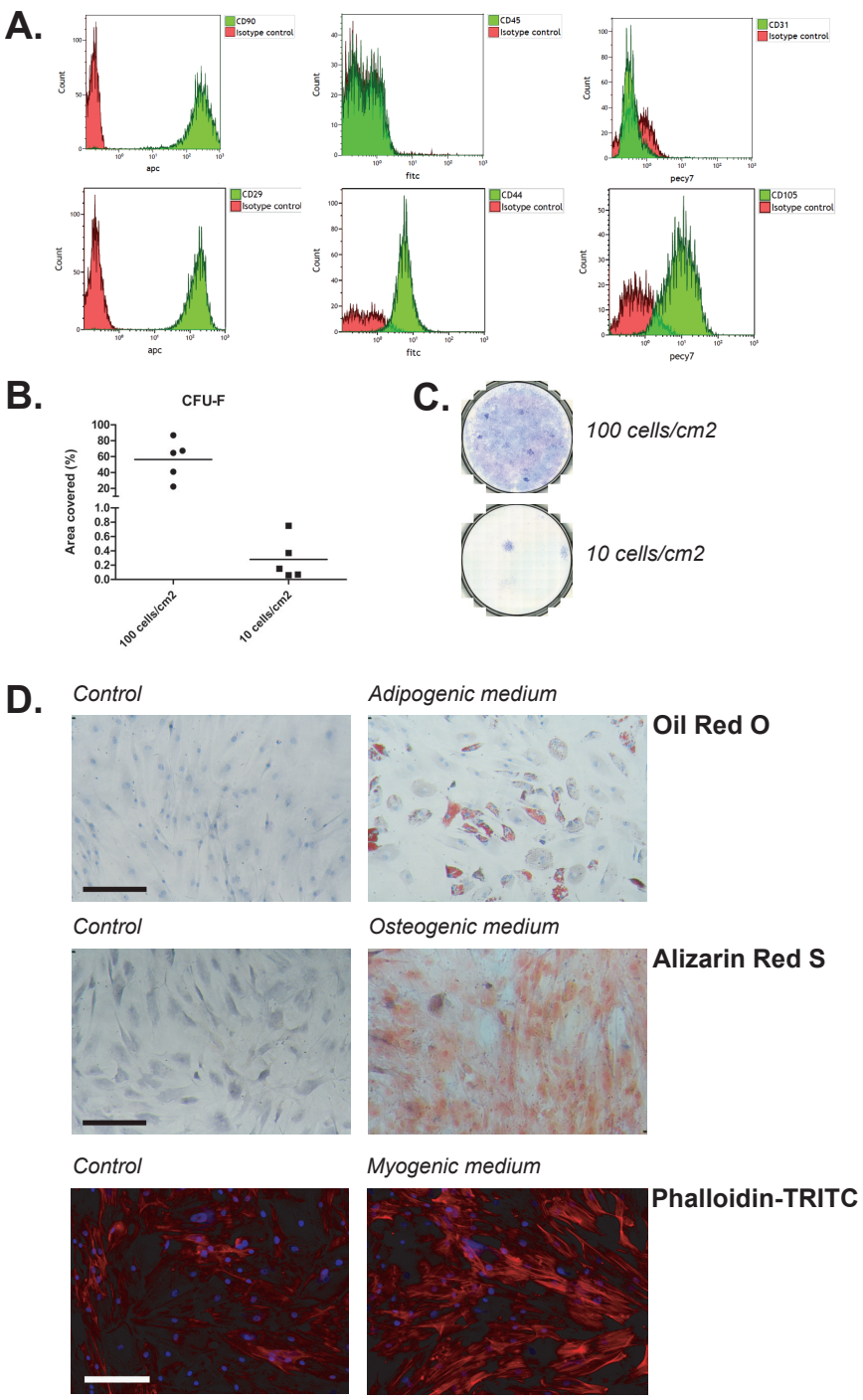

< Supplementary figure 1 | *Characterization of ASC isolated from lipoaspirates of five representative study patients. (A) FACS analysis of surface marker expression on ASC for CD90, CD45, CD31, CD29, CD44 andCD105, all compared to isotype controls. (B) Analysis of CFU-F assays of ASC plated at a density of 100 and 10 cells/mm² after fourteen days of culture (C) Representative pictures of a CFU-F culture plate with ASC plated at a density of 100 and 10 cells/mm² after fourteen days of culture. (D) Assessment of differentiation potential of ASC into adipogenic, osteogenic and myogenic lineages. Scale bars 200µm.*

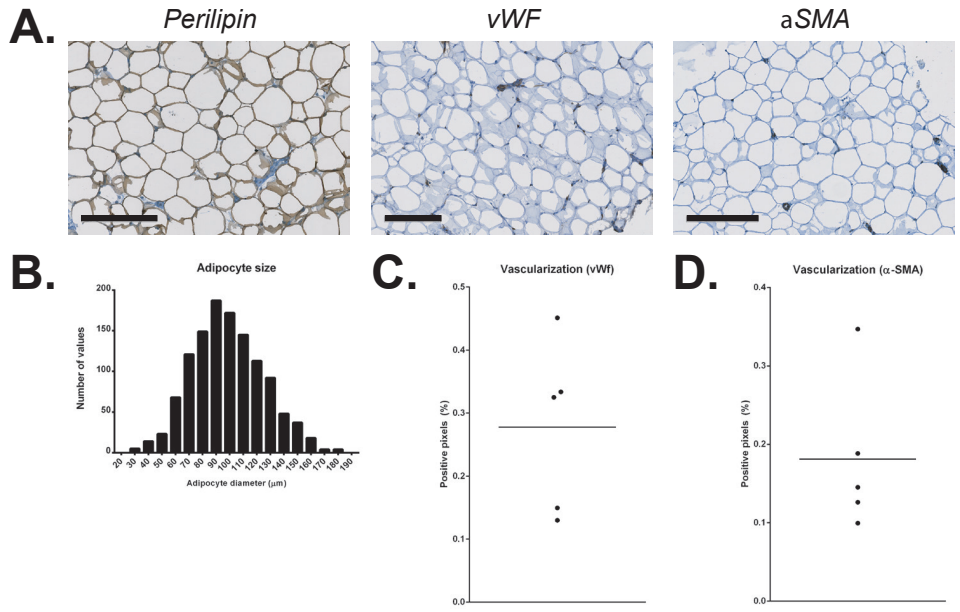

Supplementary figure 2 | Lipoaspirate histology from five representative study patients. (A) Representative pictures of immunohistochemical stainings for perilipin (for adipocytes, left panel), vWF (for endothelial cells, middle panel) and αSMA (e.g. mural cells in vessel wall, right panel). Scale bars 300 µm. (B) Quantification of adipocyte diameter in 200 adipocytes from each patient. Adipocyte size is normally distributed. Quantification of vascularization in lipoaspirate tissues by means of immunohistochemical stainings for (C) vWF and (d) αSMA.